Spatially-Variant Anisotropic Morphological Filters Driven by Gradient Fields

Rafael Verdú-Monedero[1], Jesús Angulo[2], and Jean Serra[3]

[1] Department of Information Technologies and Communications, Technical University of Cartagena, 30202, Cartagena, Spain
`rafael.verdu@upct.es`
[2] CMM-Centre de Morphologie Mathématique, Mathématiques et Systèmes, MINES Paristech, 35, rue Saint Honoré, 77305 Fontainebleau Cedex, France
`jesus.angulo@ensmp.fr`
[3] Laboratoire A2SI - ESIEE, B.P. 99, 93162 Noisy-le-Grand, France
`serraj@esiee.fr`

Abstract. This paper deals with the theory and applications of spatially-variant mathematical morphology. We formalize the definition of spatially variant dilation/erosion and opening/closing for gray-level images using exclusively the structuring function, without resorting to complement. This sound theoretical framework allows to build morphological operators whose structuring elements can locally adapt their orientation across the dominant direction of image structures. The orientation at each pixel is extracted by means of a diffusion process of the average square gradient field, which regularizes and extends the orientation information from the edges of the objects to the homogeneous areas of the image. The proposed filters are used for enhancement of anisotropic images features such as coherent, flow-like structures.

1 Introduction

The expression "spatially variant" encompasses both ideas of $i)$ the two level structure of a space E, and of all subsets $\mathcal{P}(E)$ and functions on E, and of $ii)$ some variable processing over space E. Concerning mathematical morphology, the two founding texts about point $i)$ are [16] (ch.2,3, and 9) and [7]. In [16] ch.2, devoted to the set case, Serra introduces the structuring function, with the derived four basic operations of dilation, erosion, and their two products, and the three dualities (adjunction, reciprocal and complement); it is shown that a compact structuring function may have a reciprocal version infinite everywhere. In ch.3, Matheron gives topological conditions for limiting such an expansion. Ch.9 is a first introduction to the function case, which is actually treated for the first time in [7]. In particular, Heijmans and Ronse develop the key approach by pulses sup-generators. More recent advances, due to Bouaynaya and Schonfeld can be found in [3], due to Soille in [19], and concerning Roerdink group morphology in [13]. Other papers focus specifically on efficient implementations of spatially variant morphological operators, such as those of Cuisenaire [5], Lerallut *et al.* [11] and Dokladal and Dokladalova [6].

Point ii) involves two branches. All examples in the founding papers refer to some geometrical deformation of the Euclidean space, by perspective [16] Ch.4, or by rotation invariance [7]. The perspective case corresponds to an actual application to traffic control, by Beucher *et al.* [2]. But one can imagine another mode of variability, not given by a geometrical law, but by the images under study themselves. In [17] for example, in the description of a forest fire, the structuring elements are discs whose variable radii are drawn from a so-called spread map, and they act on another image, that of the fuel map.

Rather often, spatially variant morphology is associated with the search of directions. For example, fast implementation of morphological filters along discrete lines at arbitrary angles have been reported by Soille and Talbot in [18]. Other more sophisticated algorithms for morphological operators on thin structures are the path openings of Heijmans [9]. Closer to our study, Breuß *et al.* [4] considered a PDE formulation for adaptive morphological operators and Tankyevych *et al.* [20] proposed also locally orientated operators.

In this paper we focus on linear orientated structuring elements which vary over the space according to a vector field. The originality of our approach lies in that we draw the information on the structuring elements from the image under study itself. The morphological processing is thus locally adapted to some features that already exist in the image, but that this processing aims to emphasize. Evolved filters (based on successive openings and closings) can be then used for enhancement of anisotropic images features such as coherent, flow-like structures.

In the work by Tankyevych *et al.* [20], the orientation information is computed from Hessian matrix (i.e., second-order derivatives) and the curvilinear operators, such as the morphological closing, are computed by means of reciprocal structuring functions. In this paper we show how spatially-variant anisotropic numerical openings/closings can also be computed from their direct geometric definitions. In addition, we prefer to use first-order derivatives and a diffusion-like regularization step in order to calculate the directional vector field.

The paper is organized in four parts. Section 2 sets up the morphological background. We build and describe the directional vector field from which a structuring function is generated in Section 3. With this tool in hand, we perform experiments on a series of numerical images in Section 4, measurements that are followed by the conclusion.

2   Spatially-Variant Morphology

In mathematical morphology, many usual notions are dual from each other under complement. When the variation of a structuring function follows a geometrical law, then the complement of the dilation and of the adjoint opening can be theoretically calculated. But that is no longer true for data based variation, and this drawback obliges us to express the four basic operations by means of the structuring function exclusively, without resorting to complement, or equivalently, to reciprocal dilation.

Notation. Letter E denotes an arbitrary set, which can be a digital or continuous space, or any graph. The points of E are given in bold small letters (e.g. $\mathbf{x} \in E$), and their coordinates are represented by small letters (e.g. $\mathbf{x} = (x, y)$). The subsets of E are given in capital letters (e.g. $X \subseteq E$), and the set of all these subsets (including the empty set $\varnothing$) is denoted by $\mathcal{P}(E)$. The points $\mathbf{x}$ of E, considered as elements $\{\mathbf{x}\}$ of $\mathcal{P}(E)$, are called singletons and form the sub-class $\mathcal{S}(E)$ of $\mathcal{P}(E)$. A structuring function $\delta : E \to \mathcal{P}(E)$, or equivalently from $\mathcal{S}(E)$ into $\mathcal{P}(E)$, is an arbitrary family $\{\delta(\mathbf{x})\}$ of sets indexed by the points of E. One also writes $\delta(\mathbf{x}) = B(\mathbf{x})$, for emphasizing that the transform of a point is a set.

The numerical axis $\mathcal{T}$ is an arbitrary family closed sequence of non negative numbers between two extreme bounds, 0 and M say. They can be $[0, +\infty]$, or the integers $[0, 255]$, etc. The family of all numerical functions $f : E \to \mathcal{T}$ is denoted by $\mathcal{F}(E, \mathcal{T})$. Both sets $\mathcal{P}(E)$ and $\mathcal{F}(E, \mathcal{T})$ are complete lattices, i.e., posets whose any family of elements admits a supremum (a smaller upperbound) and an infimum (a larger lowerbound) [16], [7]. For $\mathcal{P}(E)$, they are union and intersection, and for $\mathcal{F}(E, \mathcal{T})$ the pointwise sup and inf.

Dilation, erosion. Since supremum and infimum do characterize a lattice, the two basic operations that map lattice $\mathcal{P}(E)$ into itself are those which preserve either union or intersection. In mathematical morphology, they are called dilation and erosion, and denoted by δ and ε respectively:

$$\delta(\cup X_i) = \cup \delta(X_i) \quad ; \quad \varepsilon(\cap X_i) = \cap \varepsilon(X_i) \qquad X_i \in \mathcal{P}(E). \tag{1}$$

Both operations are increasing. The two families of dilations and erosions on $\mathcal{P}(E)$ correspond to each other by the Galois's relation of an adjunction, namely

$$\delta(X) \subseteq Y \quad \Leftrightarrow \quad X \subseteq \varepsilon(Y), \tag{2}$$

and given a dilation δ, there always exists one and only one erosion ε that satisfies Equivalence (2) [7].

As a set X is the union of its singletons, i.e.

$$X = \cup\{\{\mathbf{x}\} \,|\, \{\mathbf{x}\} \subseteq X\}$$

and as dilation commutes under union, this operation is generated by its restriction $\delta : \mathcal{S}(E) \to \mathcal{P}(E)$ which associates the structuring function $\delta(\mathbf{x})$ with each singleton $\{\mathbf{x}\}$ (or equivalently with each point $\mathbf{x}$ of E). The dilation of Rel.(1) becomes

$$\delta(X) = \cup\{\delta\{\mathbf{x}\}|\{\mathbf{x}\}\subseteq X\} = \cup\{\delta(\mathbf{x})|\ \mathbf{x} \in X\} = \cup\{B(\mathbf{x})|\ \mathbf{x} \in X\}. \tag{3}$$

We then draw from adjunction (2) the expression of the erosion, namely

$$\varepsilon(X) = \{\mathbf{z} \mid B(\mathbf{z}) \subseteq X\}. \tag{4}$$

In spite of the name, a dilation may not be extensive (i.e. $\delta(X) \supseteq X$). Extensivity is obtained iff for all $\mathbf{x} \in E$ we have $\mathbf{x} \in B(\mathbf{x})$. Then the adjoint erosion ε is anti-extensive.

The operation dual of dilation δ under complement is the erosion

$$\varepsilon^*(X) = [\delta(X^c)]^c,$$

whose associated structuring function is the reciprocal version of δ, i.e.

$$\mathbf{y} \in \zeta(\mathbf{x}) \qquad \text{if and only if} \qquad \mathbf{x} \in \delta(\mathbf{y}) \qquad \mathbf{x}, \mathbf{y} \in E. \qquad (5)$$

Opening and closing. Though erosion ε usually admits many inverses, the composition product

$$\gamma(X) = \delta\varepsilon(X) \qquad (6)$$

results in the smallest inverse of $\varepsilon(X)$. This product γ is increasing ($X \subseteq Y \Rightarrow \gamma(X) \subseteq \gamma(Y)$), anti-extensive ($\gamma(X) \subseteq X$) and idempotent ($\gamma\gamma(X) = \gamma(X)$). In algebra, these three features define an *opening*. Similarly, by inverting δ and ε, we obtain the *closing* $\varphi = \varepsilon\delta$, which is increasing, extensive, and idempotent.

The analytical representation of dilation δ by means of the structuring function $\mathbf{x} \to B(\mathbf{x})$ extends to the associated opening and closing. We directly draw from Relations (3) and (4) that

$$\delta\varepsilon(X) = \cup\{B(\mathbf{x})|B(\mathbf{x})\subseteq X\} \qquad (7)$$
$$\varepsilon\delta(X) = \cup\{\mathbf{x} \,|B(\mathbf{x})\subseteq \cup [B(\mathbf{x})| \; \mathbf{x} \in X]\} \qquad (8)$$

The geometrical meaning of the first relation is clear: $\delta\varepsilon(X)$ is the region of the space swept by all structuring sets $B(\mathbf{x})$ that are included in X.

Finally, Relations (3), (4), (7), and (8) that give the four basic operations are completely determined by the datum of the structuring function $\mathbf{x} \to B(\mathbf{x}) = \delta(\mathbf{x})$ and do not involve any reciprocal function. In particular, opening $\gamma = \delta\varepsilon$ and closing $\varphi = \varepsilon\delta$ are *not* dual of each other for the complement.

Dilation for numerical functions. Note that the duality under complement works for sets only, whereas adjunction duality applies to any complete lattice, such as that $\mathcal{F}(E, \mathcal{T})$ of the numerical functions that we now consider. Associated with the numerical function $f : E \to \mathcal{T}$ under study and the set structuring function $\mathbf{x} \to B(\mathbf{x})$, we introduce the following pulse function $i_{\mathbf{x},t}$ of level t at point $\mathbf{x}$

$$i_{\mathbf{x},t}(\mathbf{x}) = t \quad ; \quad i_{\mathbf{x},t}(\mathbf{y}) = 0 \quad \text{when } \mathbf{y} \neq \mathbf{x}.$$

Dilating $i_{\mathbf{x},t}$ by the structuring function B results in the cylinder $C_{B(\mathbf{x}),t}$ of base $B(\mathbf{x})$ and height t. Now, function f can be decomposed into the supremum of its pulses, i.e.

$$f = \vee\{i_{\mathbf{x},f(\mathbf{x})}, \mathbf{x} \in E\}.$$

Since dilation commutes under supremum, the dilate of f by δ, of structuring function B is given by the supremum of the dilates of its pulses, namely

$$\delta(f) = \vee\{C_{B(\mathbf{x}),f(\mathbf{x})}, \mathbf{x} \in E\}. \qquad (9)$$

Similarly, the eroded $\varepsilon(f)$ is the supremum of those pulses whose dilated cylinders are smaller than f, i.e.

$$\varepsilon(f) = \vee\{i_{\mathbf{x},t} \mid C_{B(\mathbf{x}),t} \leq f, \mathbf{x} \in E\}. \tag{10}$$

These two operations satisfy the equalities $\delta(\vee f_i) = \vee\delta(f_i)$ and $\varepsilon(\wedge f_i) = \wedge\varepsilon(f_i)$, $f_i \in \mathcal{F}$, and Galois equivalence (2) in the lattice $\mathcal{F}(E, \mathcal{T})$ of the numerical functions. Moreover, the cross sections of $\delta(f)$(resp. $\varepsilon(f)$) are the dilated (resp. the eroded) versions of the cross sections of f by the same structuring function. For this reason they are called "flat operations". Just as in the set case, the duality under adjunction does not coincide with that under the involution $f \to M - f$, which plays a role similar to a complement. The operation

$$\varepsilon^* = M - \delta(M - f)$$

turns out to still be an erosion, but ε^* is different from the ε of Rel.(10).

The two products $\gamma = \delta\varepsilon$ and $\varphi = \varepsilon\delta$ are opening and closing on $\mathcal{F}(E, \mathcal{T})$, and, as δ and ε, they commute under cross sectioning. Opening γ, for example, admits the following expression

$$\gamma(f) = \vee\{C_{B(\mathbf{x}),t} \leq f, \mathbf{x} \in E\}. \tag{11}$$

In the product space $E \times \mathcal{T}$ the subgraph of the opening $\gamma(f)$ is generated by the zone swept by all cylinders $C_{B(\mathbf{x}),t}$ smaller than f. Again, the closing $\varphi = \varepsilon\delta$ does not coincide with that, $M - \gamma(M - f)$, obtained by replacing f by $M - f$ in Rel.(11).

3   Directional Field Modelling

This section describes the method for estimating the orientation of the structures contained in a gray-level image. This vector field is obtained by using the average squared gradient and then applying a regularization process.

Average Squared gradient. The average squared gradient (ASG) method provides the directional field by squaring and averaging the gradient vectors [10,1]. Given an image $f(x, y)$, ASG uses the following definition of gradient

$$\mathbf{g} = \begin{bmatrix} g_1(x, y) \\ g_2(x, y) \end{bmatrix} = \text{sign}\left(\frac{\partial f(x,y)}{\partial x}\right) \begin{bmatrix} \frac{\partial f(x,y)}{\partial x} \\ \frac{\partial f(x,y)}{\partial y} \end{bmatrix}. \tag{12}$$

Then the gradient is squared (i.e., doubling its angle and squaring its magnitude) and averaged in some neighborhood using the window W:

$$\overline{\mathbf{g}_s} = \begin{bmatrix} \overline{g_{s,1}}(x, y) \\ \overline{g_{s,2}}(x, y) \end{bmatrix} = \begin{bmatrix} \sum_W \left(g_1^2(x, y) - g_2^2(x, y)\right) \\ \sum_W \left(2\, g_1(x, y)\, g_2(x, y)\right) \end{bmatrix}. \tag{13}$$

The directional field ASG is $\mathbf{d} = [d_1(x, y), d_2(x, y)]^\top$, where its angle is obtained as $\angle\mathbf{d} = \frac{\Phi}{2} - \text{sign}(\Phi)\frac{\pi}{2}$, which is in the range $[-\frac{\pi}{2}, \frac{\pi}{2}]$, being $\Phi = \angle\overline{\mathbf{g}_s}$; and the magnitude of $\mathbf{d}$, $||\mathbf{d}||$, can be left as the magnitude of $\overline{\mathbf{g}_s}$, or the squared root of $\overline{\mathbf{g}_s}$ or, in some applications (see e.g [12]) and in this work, it can be set to unity. In ongoing research, we consider also the use of the magnitude and coherence of directional field in order to build more general anisotropic structuring functions.

Regularization of the ASG. The vectors of the ASG field are generally different from zero only near the edges and, in homogeneous regions, where the gradient is nearly zero, the ASG is also zero. In order to extend the orientation information to pixels where the gradient is nearly zero a diffusion process is performed (similar to gradient vector flow, GVF, [21]), providing the ASG vector flow (ASGVF). The ASGVF is the vector field $\mathbf{v} = [v_1(x,y), v_2(x,y)]^\top$ that minimizes the energy functional:

$$\mathcal{E}(\mathbf{v}) = \mathcal{D}(\mathbf{v}) + \alpha \mathcal{S}(\mathbf{v}), \tag{14}$$

where $\mathcal{D}$ represents a distance measure given by the squared difference between the original and the regularized average squared gradient, weighted by the squared value of the last one,

$$\mathcal{D}(\mathbf{v}) = \frac{1}{2} \sum_{l=1}^{2} \int_E ||\mathbf{d}||^2 ||v_l - d_l||^2 \, dx \, dy, \tag{15}$$

where E is the image support and $l = 1, 2$ is the component index; the energy term $\mathcal{S}$ determines the smoothness of the directional field and represents the energy of the first order derivatives of the signal:

$$\mathcal{S}(\mathbf{v}) = \frac{1}{2} \sum_{l=1}^{2} \int_E ||\nabla v_l||^2 \, dx \, dy. \tag{16}$$

The parameter α is a regularization parameter which governs the trade-off between the smoothness and data-fidelity.

Using the calculus of variations, the ASGF field can be found by solving the following Euler equations

$$(\mathbf{v} - \mathbf{d})|\mathbf{d}|^2 - \alpha \nabla^2 \mathbf{v} = \mathbf{0}. \tag{17}$$

These equations can be solved by treating $\mathbf{v}$ as a function of time and considering the steady-state solution

$$\mathbf{v}_t + (\mathbf{v} - \mathbf{d})|\mathbf{d}|^2 - \alpha \nabla^2 \mathbf{v} = \mathbf{0}. \tag{18}$$

These equations are known as generalized diffusion equations. To set up the iterative solution, let the indices i, j, and n correspond to the discretization of x, y and t axes, respectively, and let the spacing between pixels be Δx and Δy, and the time step for each iteration be Δt. Replacing partial derivatives with its discrete approximations and considering discrete images ($\Delta x = \Delta y = 1$) gives our iterative solution to ASGF as follows:

$$v_{i,j}^{l,n} = v_{i,j}^{l,n-1} - \Delta t f_{i,j}^{l,n-1} + \frac{1}{\eta}(v_{i+1,j}^{l,n-1} + v_{i-1,j}^{l,n-1} + v_{i,j+1}^{l,n-1} + v_{i,j-1}^{l,n-1} - 4v_{i,j}^{l,n-1}) \tag{19}$$

where $f_{i,j}^{l,n-1} = (v_{i,j}^{l,n-1} - d_{i,j}^l)|\mathbf{d}_{i,j}|^2$, n is the iteration index and $\eta = (\alpha \Delta t)^{-1}$.

4   Applications and Discussion

This section shows the results of applying spatially-variant morphology operators for gray-level filtering, with a linear structuring element of fixed length λ but variable orientation. More precisely, the structuring function

$$B(\mathbf{x}) \equiv L_\lambda^{\theta(\mathbf{x})},$$

where $\theta(\mathbf{x})$ is the angle at point $\mathbf{x}$ from the regularized vector field $\mathbf{v}$. Besides erosions $\varepsilon_{L_\lambda^{\theta(\mathbf{x})}}$, dilations $\delta_{L_\lambda^{\theta(\mathbf{x})}}$, openings $\gamma_{L_\lambda^{\theta(\mathbf{x})}}$ and closings $\varphi_{L_\lambda^{\theta(\mathbf{x})}}$, we illustrate in the examples the application of alternate sequential filters (ASF): $\varphi_n\gamma_n\cdots$ $\varphi_2\gamma_2\;\varphi_1\gamma_1(f)$, or the dual version $\gamma_n\varphi_n\cdots\gamma_2\varphi_2\;\gamma_1\varphi_1(f)$. ASF present excellent properties for image denoising and regularization of dominant structures.

The present adaptive morphological filters are compared with standard translation invariant linear openings/closings which are built according to the property that the supremum (resp. infimum) of openings (resp. closings) is an opening (resp. closing) as well. The translation-invariant linear opening of size λ is given by

$$\gamma_{L_\lambda^{lines}}(f)(\mathbf{x}) = \gamma_{L^{l,\theta_1}}(f)(\mathbf{x}) \vee \gamma_{L^{l,\theta_2}}(f)(\mathbf{x}) \vee \cdots \vee \gamma_{L^{l,\theta_d}}(f)(\mathbf{x}),$$

where the following directions $\{\theta_1, \theta_2, \cdots, \theta_d\}$ are considered.

In Fig. 1 are given two synthetic images and the application of spatially-variant morphological operators. In the first example, the ASG uses a flat squared
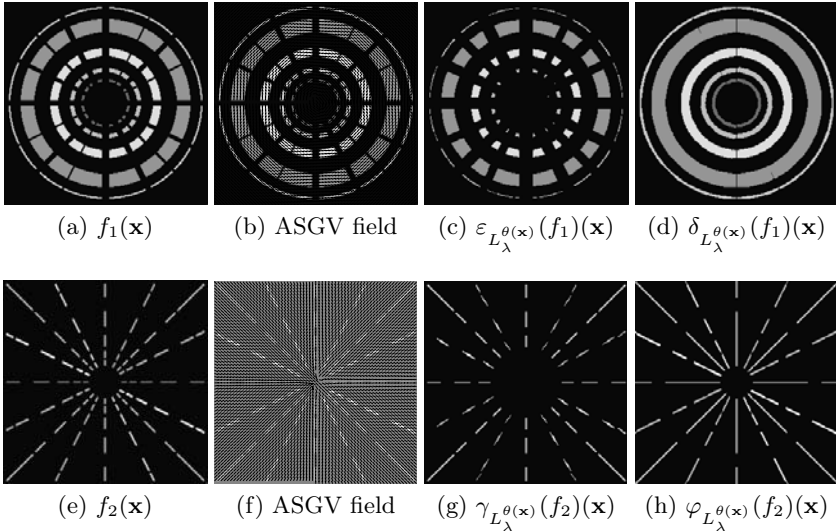

(a) $f_1(\mathbf{x})$ (b) ASGV field   (c) $\varepsilon_{L_\lambda^{\theta(\mathbf{x})}}(f_1)(\mathbf{x})$ (d) $\delta_{L_\lambda^{\theta(\mathbf{x})}}(f_1)(\mathbf{x})$

(e) $f_2(\mathbf{x})$ (f) ASGV field   (g) $\gamma_{L_\lambda^{\theta(\mathbf{x})}}(f_2)(\mathbf{x})$ (h) $\varphi_{L_\lambda^{\theta(\mathbf{x})}}(f_2)(\mathbf{x})$

Fig. 1. (a) Image "circles", (b) ASGV field using $\eta = 1$, (c) locally oriented linear erosion of length 9 pixels, (d) equivalent dilation. (e) Images "lines", (f) ASGV, $\eta = 1$, (g) locally oriented linear opening of length 11 pixels, (h) equivalent closing. Both images of size 256×256 pixels.
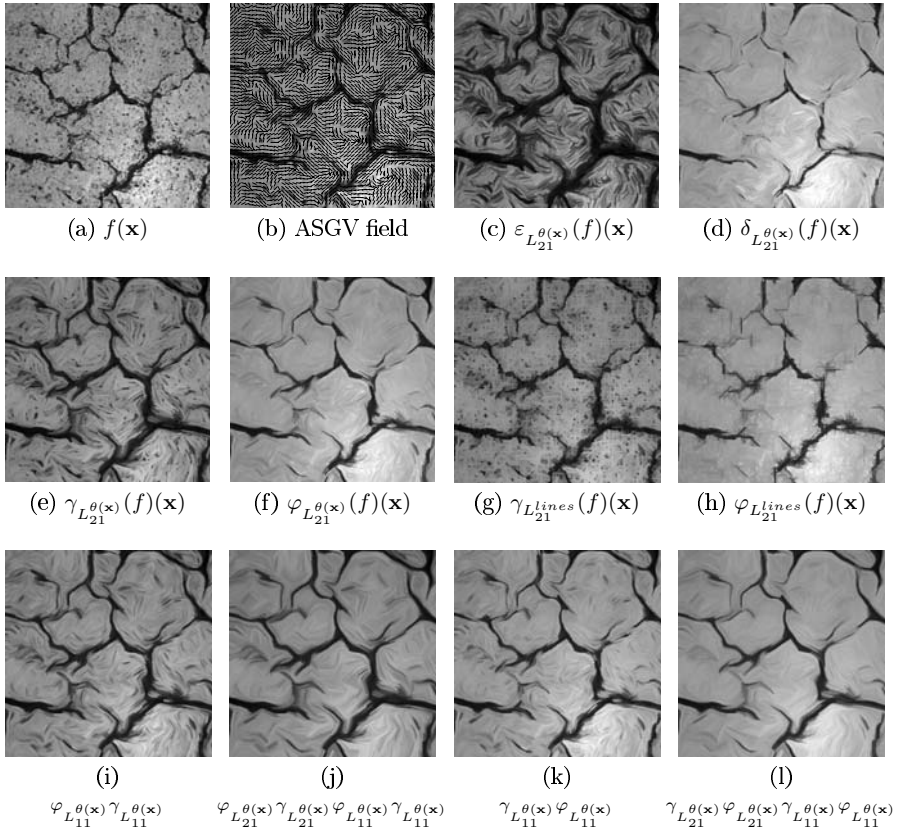
(a) $f(\mathbf{x})$ (b) ASGV field   (c) $\varepsilon_{L_{21}^{\theta(\mathbf{x})}}(f)(\mathbf{x})$ (d) $\delta_{L_{21}^{\theta(\mathbf{x})}}(f)(\mathbf{x})$

(e) $\gamma_{L_{21}^{\theta(\mathbf{x})}}(f)(\mathbf{x})$ (f) $\varphi_{L_{21}^{\theta(\mathbf{x})}}(f)(\mathbf{x})$ (g) $\gamma_{L_{21}^{lines}}(f)(\mathbf{x})$ (h) $\varphi_{L_{21}^{lines}}(f)(\mathbf{x})$

(i)   (j)   (k)   (l)
$\varphi_{L_{11}^{\theta(\mathbf{x})}}\gamma_{L_{11}^{\theta(\mathbf{x})}}$ $\varphi_{L_{21}^{\theta(\mathbf{x})}}\gamma_{L_{21}^{\theta(\mathbf{x})}}\varphi_{L_{11}^{\theta(\mathbf{x})}}\gamma_{L_{11}^{\theta(\mathbf{x})}}$ $\gamma_{L_{11}^{\theta(\mathbf{x})}}\varphi_{L_{11}^{\theta(\mathbf{x})}}$ $\gamma_{L_{21}^{\theta(\mathbf{x})}}\varphi_{L_{21}^{\theta(\mathbf{x})}}\gamma_{L_{11}^{\theta(\mathbf{x})}}\varphi_{L_{11}^{\theta(\mathbf{x})}}$

Fig. 2. (a) Original image (of size 447×447 pixels), (b) ASGV field using $\eta = 0.001$, (c) spatially-variant linear erosion of length 21 pixels, (d) spatially-variant linear dilation of length 21 pixels, (e) spatially-variant linear opening of length 21 pixels, (f) spatially-variant linear closing of length 21 pixels, (g) classical spatially-invariant linear opening of length 21 pixels (using four directions), (h) classical spatially-invariant linear opening of length 21 pixels (using four directions), (i) spatially-variant linear alternate filter (opening followed by closing) of size 11, (j) spatially-variant linear alternate sequential filter (opening followed by closing) of sizes 11 and 21, (k) spatially-variant linear alternate filter (closing followed by opening) of size 11, (l) spatially-variant linear alternate sequential filter (closing followed by opening) of sizes 11 and 21

averaging window of size 15×15, the constant of the regularization process for the ASGVF is $\eta = 1$ and the length of the structuring element is $\lambda = 9$. In the second example the window used in ASG is 11×11 pixels, η equals 1 and the structuring element is 11 pixel long. We can remark the appropriateness of very simple morphological filters for closing interrupted line structures and for the suppression of line structures of small size. As expected, the results are
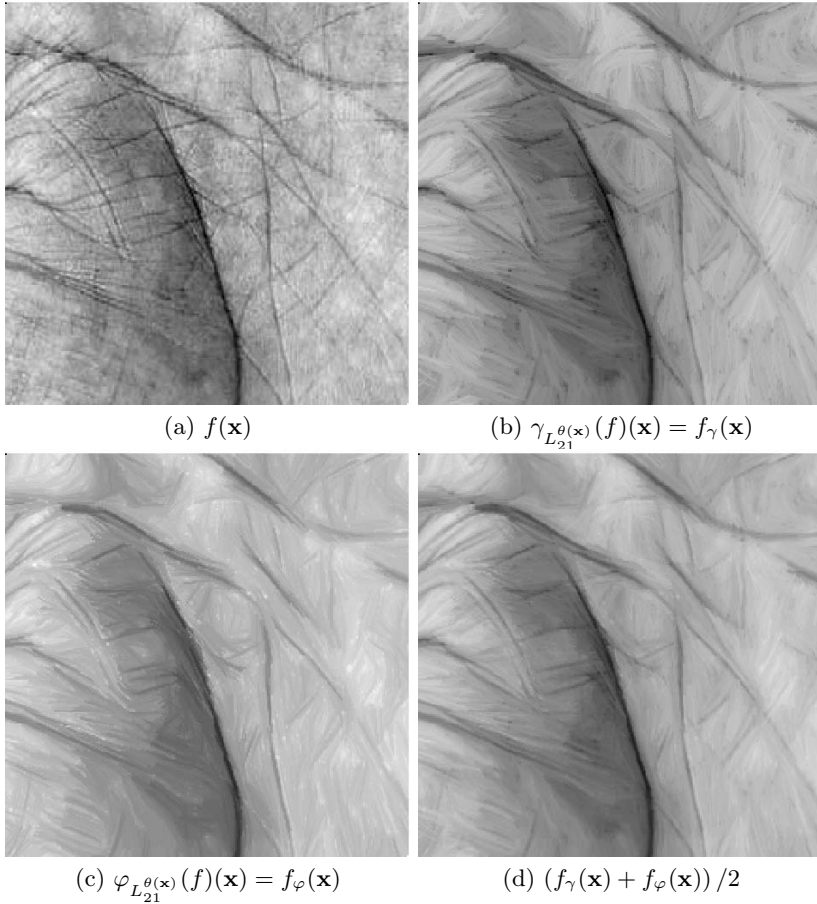
<table>
<tr><td>(a) $f(\mathbf{x})$</td><td>(b) $\gamma_{L_{21}^{\theta(\mathbf{x})}}(f)(\mathbf{x}) = f_\gamma(\mathbf{x})$</td></tr>
<tr><td>(c) $\varphi_{L_{21}^{\theta(\mathbf{x})}}(f)(\mathbf{x}) = f_\varphi(\mathbf{x})$</td><td>(d) $(f_\gamma(\mathbf{x}) + f_\varphi(\mathbf{x}))/2$</td></tr>
</table>

Fig. 3. (a) Original image (of size 256×256 pixels), (b) spatially-variant linear opening of length 21 pixels, (c) spatially-variant linear closing of length 21 pixels, (d) average image between the spatially-variant linear opening and closing. The ASGV field has been computed using $\eta = 0.01$.

quite spatially regular and only a negligible number of points propagate values according to wrong directions.

The example depicted in Fig. 2 is a real world image, presenting a network of coherent, flow-like structures on a very irregular background. The window used in ASG is 21×21 pixels, $\eta = 0.001$. We have studied the proposed filters for enhancement of anisotropic image features. In particular, it is shown how the ASF produce very interesting anisotropic effects. It is evident in this case that the closing (or the ASF starting by a closing) is more appropriate because the target structures are darker than their background. We can also compare the new spatially-variant linear opening/closing with their counterpart classical spatially-invariant linear opening/closing.

Fig. 3 provides a last case of morphological anisotropic filtering. For this example, the window used in ASG is 21×21 pixels, $\eta = 0.01$. The original image represents a hand palm and the aim of the filtering step is to enhance the main lines which are the most important for biometric identification. A pair of spatially-variant linear opening and closing are compared with the average images of both operators. As we can observe, the average image is a good trade-off between these two basic morphological anisotropic filters and the result is quite regular but preserves the significant linear structures.

One of the key points for the good results of these anisotropic filters is the computation of the gradient field. In the three examples, the value of the time step of the regularization process is $\Delta t = 1$. The size of the averaging window has been taken in order to preserve the orientation of the main structures in the images: circles or lines in Fig. 1, big crevices in Fig. 2) and main lines in Fig. 3), without affecting the presence of gaps in the lines and circles nor the small spots/crevices/lines. For example, in Fig. 1-bottom, the lines have a width of 3 pixels, therefore computing the ASG with an averaging window of size greater than 3×3 will preserve the main orientation of the lines ignoring the gaps. In the regularization process, the parameter η is related to the bandwidth of a low-pass filter which filters the increments of ASGVF in Eq. (19). When the gradient of the image has homogeneous areas and abrupt transitions (as it happens in the first synthetic image) a higher value is necessary to allow abrupt transitions (spatial high frequencies) exist. On the other hand, when the gradient has not abrupt transitions a low value of η gets the appropriate smoothness in the regularized vector field (as happens in Fig. 2 and 3).

5   Conclusion and Perspectives

We have clarified and solved some difficulties in the definition of spatially variant dilation/erosion and opening/closing for gray-level images. Then, we have proposed an algorithm for a reliable extraction of orientation information, which is finally used to build linear anisotropic morphological filters. The performance of derived operators has been illustrated for enhancement of anisotropic images features such as coherent, flow-like structures.

In ongoing research, we would like to address the theory of spatially-variant geodesic operators. From a practical viewpoint, we are working on a full exploitation on the directional field, including the information of magnitude and angular coherence in order to propose more general anisotropic structuring elements, not limited to orientated lines of fixed length. The extension to 3-D and more generally to n-D spaces and the application to 3-D images (e.g., denoising MRI data, enhancement of fiber networks, etc.) will be also explored in future work.

References

1. Bazen, A.M., Gerez, S.H.: Systematic methods for the computation of the directional fields and singular points of fingerprints. IEEE Trans. Pattern Anal. Mach. Intell. 24(7), 905–919 (2002)
2. Beucher, S., Blosseville, J.M., Lenoir, F., Motyka, V., Kraft, C.: TITAN, a traffic measurement system using image processing techniques. In: Proceedings IEE Road Traffic Congress (1989)
3. Bouaynaya, N., Schonfeld, D.: Theoretical foundations of spatially-variant mathematical morphology part II: Gray-level images. IEEE Trans. Pattern Anal. Mach. Intell. 30, 837–850 (2008)
4. Breuß, M., Burgeth, B., Weickert, J.: Anisotropic continuous-scale morphology. In: Martí, J., Benedí, J.M., Mendonça, A.M., Serrat, J. (eds.) IbPRIA 2007, Part II. LNCS, vol. 4478, pp. 515–522. Springer, Heidelberg (2007)
5. Cuisenaire, O.: Locally adaptable mathematical morphology using distance transformations. Pattern Recognition 39, 405–416 (2006)
6. Dokladal, P., Dokladalova, E.: Grey-scale Morphology with Spatially-Variant Rectangles in Linear Time. In: Blanc-Talon, J., Bourennane, S., Philips, W., Popescu, D., Scheunders, P. (eds.) ACIVS 2008. LNCS, vol. 5259, pp. 674–685. Springer, Heidelberg (2008)
7. Heijmans, H.J.A.M., Ronse, C.: The algebraic basis of mathematical morphology - part I: Dilations and erosions. Computer Vision, Graphics and Image Processing 50, 245–295 (1990)
8. Heijmans, H.J.A.M.: Morphological Image Operators. Academic Press, Boston (1994)
9. Heijmans, H., Buckley, M., Talbot, H.: Path openings and closings. Journal of Mathematical Imaging and Vision 22, 107–119 (2005)
10. Kass, M., Witkin, A.: Analyzing oriented patterns. Comput. Vision Graph. Image Process. 37(3), 362–385 (1987)
11. Lerallut, R., Decenciére, E., Meyer, F.: Image filtering using morphological amoebas. Image Vision Comput. 25, 395–404 (2007)
12. Perona, P.: Orientation diffusions. IEEE Trans. Image Processing 7(3), 457–467 (1998)
13. Roerdink, J.: Group morphology. Pattern Recognition 33, 877–895 (2000)
14. Ronse, C., Heijmans, H.J.A.M.: The algebraic basis of mathematical morphology - part II: Openings and closings. Computer Vision, Graphics and Image Processing: Image Understanding 54, 74–97 (1991)
15. Serra, J.: Image Analysis and Mathematical Morphology, vol. I. Academic Press, London (1982)
16. Serra, J.: Image Analysis and Mathematical Morphology: Theoretical Advances, vol. II. Academic Press, London (1988)
17. Serra, J., Suliman, M.D.H., Mahmud, M.: Prediction of Scars in Malaysian Forest fires by means of Random Spreads. In: Proc. of Int. ISPRS Conf. on Techniques and Applications of Optical and SAR Imagery fusion (2007)
18. Soille, P., Talbot, H.: Directional morphological filtering. IEEE Trans. Pattern Anal. Mach. Intell. 23, 1313–1329 (2001)
19. Soille, P.: Morphological image analysis. Springer, Heidelberg (1999)
20. Tankyevych, O., Talbot, H., Dokladal, P.: Curvilinear Morpho-Hessian Filter. In: Proceedings of ISBI 2008, pp. 1011–1014 (2008)
21. Xu, C., Prince, J.L.: Generalized gradient vector flow external forces for active contours. Signal Processing 71(2), 131–139 (1998)